International Journal of
ROBOTICS & AUTOMATION

VOLUME 14, Number 4, 1999

ISSN 0826-8185

Published by ACTA Press ANAHEIM * CALGARY * ZURICH

International Journal of Robotics and Automation, Vol. 14, No. 4, 1999

LYAPUNOV-BASED SET POINT CONTROL OF THE ACROBOT

E. Zergeroglu,* W.E. Dixon,* D.M. Dawson,* and A. Behal*

Abstract

In this paper, we present an alternative approach for set point control of the acrobot. The primary control objective is to regulate the first link at any desired position. A Lyapunov-based control algorithm, which is applicable to both the directly driven and the remotely driven acrobot, is proposed. The controller ensures that the first link is asymptotically driven to the desired set point, provided some sufficient conditions on the controller gains and the physical parameters are satisfied. Both simulation and experimental results are presented to illustrate the performance of the proposed control law.

Key Words

Underactuated systems, robot manipulators, nonlinear control

1. Introduction

While many established nonlinear control schemes have been developed for fully actuated mechanical systems (e.g., robot manipulators), there does not seem to be a consensus with regard to nonlinear control solutions for underactuated systems (e.g., inverted pendulum, acrobot, etc.). Due to its underactuated nature and highly nonlinear dynamics, control of the two-degree freedom acrobot has become one of the benchmark control design problems for underactuated systems. In the past, the two acrobot configurations that are primarily discussed in the literature are the *directly driven* acrobot and the *remotely driven* acrobot. The directly driven acrobot (i.e., see [1]) is characterized by the control torque being applied directly to the second link while the remotely driven acrobot (i.e., see [2]–[4]) is characterized by the control torque being applied between the two links.

Much of the previous acrobot control research focused primarily on applying linearization techniques. For example, in [1], Hauser et al. used an approximate nonlinear model that is full state linearizable while Spong [2] presented swing-up control algorithms based on partial feedback linearization. In [3], Bortoff presented a technique for the construction of a pseudo-linear controller that is intimately related to extended linearization and gain scheduling (i.e., a nonlinear function of the state is used to schedule the gains of a linear controller among a continuum of operating points). In [4] Davidson et al. introduced a state feedback linearizing controller which uses spline function-based interpolation to construct the controller. In [5] and [6], Boone presented both optimal control and intelligent control techniques for the control of the acrobot.

In this paper, our primary control objective is to asymptotically position the first link of the acrobot at any desired angular position. To faciliate this control objective, we introduce a counterweight connected to the first link of the acrobot to allow the acrobot to balance in every position. To achieve the control objective, we use a Lyapunov-based approach that: 1) utilizes a saturated feedback torque input control, 2) uses a desired set point position for the second link, and 3) restricts the value for the counter-weight to be within a certain range. These three elements of the design work together to ensure that the first link is driven to the desired position and ensure that all signals remain bounded during closed-loop operation. This paper is organized in the following manner. Section 2 describes the dynamic models for both the directly driven and remotely driven acrobot configurations and presents some associated properties used in control development. Section 3 presents the control formulation and stability analysis. Simulation and experimental results are presented in Section 4 and Section 5, respectively. Section 6 contains some concluding remarks.

2. Mathematical Model

The mathematical model for the two-link robotic system, known as the acrobot, can be written using the Euler-Lagrange formulation described in [7] as follows:

$$M(q)\ddot{q} + V_m(q,\dot{q})\dot{q} + F_d\dot{q} + G(q) = K\tau \qquad (1)$$

where $q(t)$, $\dot{q}(t)$, and $\ddot{q}(t) \in \Re^2$ denote the link position, velocity, and acceleration, respectively, $M(q) \in \Re^{2\times 2}$, $V_m(q,\dot{q}) \in \Re^{2\times 2}$, and $G(q) \in \Re^2$ represent the inertia matrix, centripetal-Coriolis matrix, and the gravitational vector, respectively, $F_d \in \Re^{2\times 2}$ denotes the constant diagonal matrix of viscous friction coefficients, $\tau \in \Re^1$ is the torque control input, and $K \in \Re^2$ is a transmission vector explicitly defined as follows:

* Department of Electrical & Computer Engineering, Clemson University, Clemson, SC 29634-0915, USA; e-mails: [ezerger, wdixon, ddawson, abehal]@ces.clemson.edu

(paper no. 98-024)

$$K = \begin{bmatrix} 0 & 1 \end{bmatrix}^T \text{ for the directly driven acrobot}$$
$$K = \begin{bmatrix} k_1 & k_2 \end{bmatrix}^T \text{ for the remotely driven acrobot} \quad (2)$$

where k_1 and k_2 are constants that depend on the properties of the mechanical elements used for torque transmission (i.e., pulleys, belts, etc.).

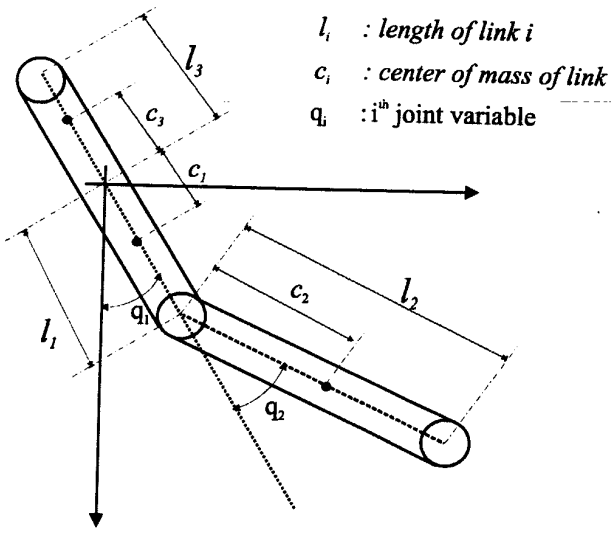

Figure 1. Acrobot, coordinate reference frames.

From Fig. 1, we can derive the expressions for the components of the inertia matrix as follows:

$$\begin{aligned} M_{11} &= m_1 c_1^2 + m_2 l_1^2 + m_2 c_2^2 + 2 m_2 l_1 c_2 \cos(q_2) \\ &\quad + m_3 c_3^2 + I_1 + I_2 + I_3 \\ M_{12} = M_{21} &= m_2 c_2^2 + m_2 l_1 c_2 \cos(q_2) + I_2 \\ M_{22} &= m_2 c_2^2 + I_2 \end{aligned} \quad (3)$$

where M_{ij} represents the ij-th component of the inertia matrix, and m_i, c_i, l_i, and I_i denote the mass, center of mass, length, and inertia for link 1, link 2, and the counter-weight ($i = 3$), respectively. From Fig. 1, we can also obtain expressions for the centripetal-Coriolis matrix and the gravitational vector as follows:

$$V_m(q, \dot{q}) = \begin{bmatrix} -m_2 l_1 c_2 \sin(q_2)\dot{q}_2 & -m_2 l_1 c_2 \sin(q_2)(\dot{q}_1 + \dot{q}_2) \\ m_2 l_1 c_2 \sin(q_2)\, \dot{q}_1 & 0 \end{bmatrix} \quad (4)$$

and:

$$G(q) = \begin{bmatrix} (g_1 - g_3)\sin(q_1) + g_2 \sin(q_1 + q_2) \\ g_2 \sin(q_1 + q_2) \end{bmatrix} \quad (5)$$

where the constants g_1, g_2, and g_3 are given by:

$$g_1 = (m_1 c_1 + m_2 l_1) g \; g_2 = (m_2 c_2) g \; g_3 = (m_3 c_3) g \quad (6)$$

and g denotes the gravitational constant. From the definitions given in (3) and (4), the standard skew symmetric relationship between the inertia and centripetal-Coriolis matrices is given as follows:

$$v^T \left(\frac{1}{2} \dot{M}(q) - V_m(q, \dot{q}) \right) v = 0 \quad \forall v \in \Re^2 \quad (7)$$

where $\dot{M}(q)$ denotes the time derivative of the inertia matrix. As an aid in the subsequent analysis, we also note that the gravitational energy of the system shown in Fig. 1 can be defined as follows:

$$\begin{aligned} U(q) &= g_1 (1 - \cos(q_1)) \\ &\quad + g_2 (1 - \cos(q_1 + q_2)) + g_3 (1 + \cos(q_1)) \end{aligned} \quad (8)$$

where the partial derivative of $U(q) \in \Re^1$ with respect to $q(t)$ is equal to the gravitational vector as shown below:

$$\frac{\partial U(q)}{\partial q} = G(q) = \left[\frac{\partial U(q)}{\partial q_1} \;\; \frac{\partial U(q)}{\partial q_2} \right]^T \quad (9)$$

3. Control Development

The primary objective is to design a controller that regulates the first link of the acrobot to any desired constant position. In order to unify the development for both the remotely driven and the directly driven acrobot, we define a new state variable $y(t) \in \Re^2$ as follows:

$$y = \begin{bmatrix} y_1 \\ y_2 \end{bmatrix} = S^{-1} q \quad (10)$$

where $y_1(t)$ and $y_2(t)$ denote the elements of $y(t)$, $S \in \Re^{2 \times 2}$ is a constant, nonsingular transformation matrix defined as follows:

$$S = \begin{bmatrix} s_{11} & 0 \\ s_{21} & s_{22} \end{bmatrix} \quad (11)$$

and the elements s_{11}, s_{21}, and s_{22} are selected to satisfy the following equality:

$$S^T K = \begin{bmatrix} 0 \\ 1 \end{bmatrix} \quad (12)$$

where K was defined in (2). In addition to satisfying (12), the subsequent stability analysis requires that the elements s_{11}, s_{21}, and s_{22} be selected to satisfy the following inequality:

$$0 < \left| \left(\frac{s_{11}}{s_{11} + s_{21}} \right) \right| < 1 \quad (13)$$

A particular choice for the matrix S which is nonsingular and satisfies (12) is given below:

$$S = \begin{bmatrix} k_2 & 0 \\ -k_1 & \frac{1}{k_2} \end{bmatrix} \quad (14)$$

It also important to note that the choice for S given by (14) also satisfies (13) since for our acrobot and for the acrobot given in [3], k_1 is a negative number, and k_2 is a positive number.

After premultiplying both sides of (1) by S^T and utilizing (10), we can obtain the following transformed dynamic equation for the acrobot:

$$S^T M(y) S\ddot{y} + S^T V_m(y,\dot{y}) S\dot{y} + S^T F_d S\dot{y} + S^T G(y) = S^T K\tau \quad (15)$$

Motivated by the structure of (15), and the desire to obtain a dynamic model similar to (1), we define $M^*(y) = S^T M(y) S$, $V_m^*(y,\dot{y}) = S^T V_m(y,\dot{y}) S$, $F^* = S^T F S$, and $G^*(y) = S^T G(y)$, in order to rewrite (15) as follows:

$$M^*(y)\ddot{y} + V_m^*(y,\dot{y})\dot{y} + F^*\dot{y} + G^*(y) = \begin{bmatrix} 0 \\ 1 \end{bmatrix} \tau \quad (16)$$

where (12) has been utilized, $G^*(y)$ is explicitly given by:

$$G^*(y) = \begin{bmatrix} G_1^*(y) \\ G_2^*(y) \end{bmatrix} \quad (17)$$

and the auxiliary functions $G_1^*(y)$ and $G_2^*(y)$ are defined by:

$$G_1^*(y) = s_{11}\left(\sin s_{11} y_1\right)(g_1 - g_3)$$
$$+ (s_{11} + s_{21})\, g_2 \sin\left(s_{11} y_1 + s_{21} y_1 + s_{22} y_2\right) \quad (18)$$

$$G_2^*(y) = s_{22} g_2 \sin\left(s_{11} y_1 + s_{21} y_1 + s_{22} y_2\right) \quad (19)$$

Remark 1: Since S is defined as a constant, nonsingular matrix, it is trivial to show that the skew-symmetric property defined in Property 1 still holds for the transformed dynamic model given in (16). In addition, we note that it is easy to show that $M^*(y)$ and F^* are positive definite, symmetric matrices. Furthermore, according to (9), we can define the following relationship $\frac{\partial U^*(y)}{\partial y} = G^*(y)$ where $U^*(y)$ denotes the gravitational energy of the system in terms of $y(t)$ and is explicitly given by:

$$U^*(y) = g_1\left(1 - \cos(s_{11} y_1)\right)$$
$$+ g_2\left(1 - \cos(s_{11} y_1 + s_{21} y_1 + s_{22} y_2)\right)$$
$$+ g_3\left(1 + \cos(s_{11} y_1)\right) \quad (20)$$

Hereinafter, the control development and the stability analysis will be performed on the transformed remotely driven acrobot dynamics given by (16).

3.1 Control Formulation

Given a desired constant set point position for link 1 (denoted by q_{d1}), our primary control design objective is the design of a torque control input $\tau(t)$ to ensure that the actual position of link 1 is asymptotically regulated to q_{d1}. To achieve the primary control design objective, we also design a desired set point position for link 2 (denoted by q_{d2}) and restrict the value for the counter-weight g_3 to be within a certain range. According to the transformation given by (10), we define the desired set point for the variable $y(t)$ as follows:

$$y_d = S^{-1} q_d \quad (21)$$

where q_d and $y_d \in \Re^2$ are explicitly defined as follows:

$$y_d = \begin{bmatrix} y_{d1} \\ y_{d2} \end{bmatrix} \quad q_d = \begin{bmatrix} q_{d1} \\ q_{d2} \end{bmatrix} \quad (22)$$

From (21) and (11), it is a straightforward matrix operation to show that:

$$\begin{bmatrix} y_{d1} \\ y_{d2} \end{bmatrix} = \begin{bmatrix} \frac{q_{d1}}{s_{11}} \\ -\frac{s_{21} q_{d1}}{s_{11} s_{22}} + \frac{q_{d2}}{s_{22}} \end{bmatrix} \quad (23)$$

Based on the transformed dynamics given in (16), the above transformation given by (21), and the subsequent stability analysis, we define the control torque input for the remotely driven acrobot as follows:

$$\tau = G_2^*(y_d) - k_p \tanh(y_2 - y_{d2}) - k_v \dot{y}_2 \quad (24)$$

where k_p and $k_v \in \Re^1$ are positive controller gains, $G_2^*(\cdot)$ was defined in (19), and y_{d2} is defined as follows:

$$y_{d2} = \frac{1}{s_{22}} \sin^{-1}\left\{\left(\frac{g_3 - g_1}{g_2}\right)\left(\frac{s_{11}}{s_{11} + s_{21}}\right)\sin(s_{11} y_{d1})\right\}$$
$$- \frac{s_{11} + s_{21}}{s_{22}} y_{d1} \quad (25)$$

the g_i's were defined in (6), and y_{d1} is given by (23). To ensure that a solution for y_{d2} exists, we require that the value for the counter-weight g_3 be designed to satisfy the following condition:

$$0 < |A| < 1 \quad (26)$$

where the constant A is defined as follows:

$$A = \left(\frac{g_3 - g_1}{g_2}\right)\left(\frac{s_{11}}{s_{11} + s_{21}}\right) \quad (27)$$

After substituting (24) into (16), we obtain the following closed-loop system:

$$M^*(y)\ddot{y} + V_m^*(y,\dot{y})\dot{y} + F^*\dot{y} + G^*(y)$$
$$= \begin{bmatrix} 0 \\ G_2^*(y_d) - k_p \tanh(y_2 - y_{d2}) - k_v \dot{y}_2 \end{bmatrix} \quad (28)$$

Remark 2: It is easy to show that (10) and (23) can be used to rewrite the controller given by (24) and (25) in terms of the joint space variables as follows:

$$\tau = g_2 s_{22} \sin(q_{d1} + q_{d2}) - k_v \left(-\frac{s_{21}}{s_{11} s_{22}} \dot{q}_1 + \frac{1}{s_{22}} \dot{q}_2 \right)$$

$$-k_p \tanh \left(-\frac{s_{21}}{s_{11} s_{22}} (q_1 - q_{d1}) + \frac{1}{s_{22}} (q_2 - q_{d2}) \right) \quad (29)$$

For the directly driven acrobot, the S matrix defined in (11) is the 2×2 identity matrix; hence, according to (11) and (29), the corresponding control input for the directly driven acrobot is given by:

$$\tau = g_2 \sin(q_{d1} + q_{d2}) - k_p \tanh(q_2 - q_{d2}) - k_v \dot{q}_2 \quad (30)$$

We note that the condition given by (13) is not required during the stability analysis for the directly driven acrobot.

3.2 Stability Analysis

Theorem 1: Given the dynamic equation for the remotely driven acrobot in (16), the proposed controller given in (24) and (25) ensures global asymptotic set point regulation in the sense that:

$$\lim_{t \to \infty} q_1(t) = q_{d1} \quad (31)$$

if the S matrix defined in (11) satisfies the condition given by (13), the value for the counter-weight g_3 is designed to satisfy (26), and the control gain k_p is selected according to:

$$k_p > \max \{\gamma_1, \gamma_3\} \quad (32)$$

where γ_1 and γ_3 are scalar constants defined as follows:

$$\gamma_1 = \left| (g_3 - g_1) \left(\frac{s_{11} s_{22} \pi}{s_{11} + s_{21}} \right) \right| \quad (33)$$

and:

$$\gamma_3 = \left| \frac{s_{11}^2 s_{22}^2 (g_3 - g_1) g_2}{\varrho} \right| \quad (34)$$

where axiliary variable ϱ is defined as:

$$\varrho = (g_1 - g_3) s_{11}^2 \cos(s_{11} y_{d_1})$$
$$+ g_2 (s_{11} + s_{21})^2 \cos((s_{11} + s_{21}) y_{d1} + s_{22} y_{d2})$$

Proof: In order to prove Theorem 1, we utilize the following nonnegative function:

$$V = \frac{1}{2} \dot{y}^T M^*(y) \dot{y} + P(y) \quad (35)$$

where the potential energy-like function $P(y)$ is defined as:

$$P(y) = U^*(y) - y^T G^*(y_d) - (U^*(y_d) - y_d^T G^*(y_d))$$
$$+ k_p \ln (\cosh (y_2 - y_{d2})) \quad (36)$$

$G^*(y)$ was defined in (17), and $U^*(y)$ was defined in (20). Utilizing Lemma A.1 in Appendix A, we show that if the control gain k_p is selected according to (32) then $P(y) \geq 0$; thus, $V(t)$ is nonnegative. After taking the time derivative of (35), substituting (36) and (28), and employing the skew-symmetry property given in (7), we have the following expression:

$$\dot{V} = -\dot{y}^T F^* \dot{y} - \dot{y}^T G^*(y)$$
$$+ \dot{y}^T \begin{bmatrix} 0 \\ G_2^*(y_d) - k_p \tanh(y_2 - y_{d2}) - k_v \dot{y}_2 \end{bmatrix}$$
$$+ \dot{y}^T \frac{\partial U^*(y)}{\partial y} - \dot{y}^T G^*(y_d) + k_p \tanh(y_2 - y_{d2}) \dot{y}_2 \quad (37)$$

After recalling that $\frac{\partial U^*(y)}{\partial y} = G^*(y)$ (see (17) and (20)), utilizing (10) and (17), we can simplify the expression for $\dot{V}(t)$ of (37) to yield:

$$\dot{V} = -\dot{y}^T F^* \dot{y} - k_v \dot{y}_2^2 - \dot{y}_1 G_1^*(y_d) \quad (38)$$

From (18) and (25), it is apparent that y_{d2} has been selected to ensure that $G_1^*(y_d) = 0$; hence, we can upper bound $\dot{V}(t)$ of (38) as follows:

$$\dot{V} \leq -F^* \|\dot{y}\|^2 \quad (39)$$

As a result of (39), $V(t)$ of (35) must be decreasing or constant; therefore, since $V(t)$ is nonnegative, we know that $V(t) \in \mathcal{L}_\infty$. Since $V(t) \in \mathcal{L}_\infty$, we can see from (35), (36), and Lemma A.1 in Appendix A that $\dot{y}(t) \in \mathcal{L}_\infty^2$ (note $M^*(y)$ is positive definite). From the saturated feedback structure of $\tau(t)$ given in (24) and the fact that $\dot{y}(t) \in \mathcal{L}_\infty$, we can see that $\tau(t) \in \mathcal{L}_\infty$. From the structure of the dynamics given in (16) (i.e., $M^*(y)$ is invertible and bounded for all $y(t)$, $V_m^*(y, \dot{y})$ is bounded for all $y(t)$ and bounded $\dot{y}(t)$, F^* is a constant matrix, and $G^*(y)$ is always bounded), we have $\ddot{y}(t) \in \mathcal{L}_\infty^2$ (i.e., $\dot{y}(t)$ is uniformly continuous) since $\dot{y}(t) \in \mathcal{L}_\infty^2$, $\tau(t) \in \mathcal{L}_\infty$. After taking the time derivative of (28), we can also show in a similar manner that $\dddot{y}(t) \in \mathcal{L}_\infty^2$ (i.e., $\ddot{y}(t)$ is uniformly continuous) since $\dot{y}(t)$, $\ddot{y}(t) \in \mathcal{L}_\infty^2$. Since $V(t) \in \mathcal{L}_\infty$, it is now a straightforward manner to show that $\dot{y}(t) \in \mathcal{L}_2^2$; hence, since $\dot{y}(t)$, $\ddot{y}(t) \in \mathcal{L}_\infty^2$, and $\dot{y}(t) \in \mathcal{L}_2^2$, we can apply a corollary to Barbalat's Lemma [8] to show that $\lim_{t \to \infty} \dot{y}(t) = 0$. Since $\lim_{t \to \infty} \dot{y}(t) = 0$ and $\ddot{y}(t)$ is uniformly continuous, we can directly apply Barbalat's Lemma [8] to show that $\lim_{t \to \infty} \ddot{y}(t) = 0$. Since $\lim_{t \to \infty} \dot{y}(t)$, $\ddot{y}(t) = 0$, we can pass the limit on the closed-loop system given in (28) to obtain:

$$\lim_{t \to \infty} \{ s_{11} (\sin s_{11} y_1) (g_1 - g_3)$$
$$+ (s_{11} + s_{21}) g_2 \sin (s_{11} y_1 + s_{21} y_1 + s_{22} y_2) \} = 0 \quad (40)$$

$$\lim_{t \to \infty} \{ s_{22} g_2 \sin (s_{11} y_1 + s_{21} y_1 + s_{22} y_2)$$
$$- s_{22} g_2 \sin (s_{11} y_{d1} + s_{21} y_{d1} + s_{22} y_{d2}) + k_p \tanh(y_2 - y_{d2}) \}$$
$$= 0 \quad (41)$$

In Lemma A.1 of Appendix A, we show that if the control gain k_p is selected according to (32), then the only solution for (40) and (41) is:

$$\lim_{t\to\infty}(y - y_d) = 0 \tag{42}$$

Now according to (10) and (21), we have:

$$q - q_d = S(y - y_d) \tag{43}$$

hence, since the matrix S is defined to be nonsingular as given by (14), the result given by (31) follows directly from (42) and (43). QED

Remark 3: As mentioned in Remark 2, the S matrix defined in (11) is selected as the 2×2 identity matrix, and the control is given by (30) for the directly driven acrobot. By following the same steps outlined in the proof of Theorem 1, we obtain the same stability result as that given by (31) for the directly driven acrobot provided the value for the counter-weight g_3 is designed to satisfy (26), and the control gain k_p is selected according to (32). We again note that the condition given by (13) is not required during the stability analysis for the directly driven acrobot.

Remark 4: As far as we know, all of the previous control algorithms for the acrobot required link position and link velocity measurements. It should be noted that the requirement for link velocity measurements can be eliminated by using a similar method as that given in [9]. Specifically, we redefine the torque control input given by (24) as follows:

$$\tau = G_2^*(y_d) - k_p \tanh(y_2 - y_{d2}) - k_v\xi \tag{44}$$

where $\xi(t) \in \Re^1$ is a surrogate for link velocity measurements that is generated by the following filter:

$$\dot{p} = -p - y_2 \tag{45}$$

$$\xi = p + y_2 \tag{46}$$

where $p(t) \in \Re^1$ is an auxiliary filter variable which allows $\xi(t)$ to be calculated with only link position measurements. It is easy to show that the auxiliary filter variable $p(t)$ can be eliminated from (44) and (45) to yield the following equivalent dynamical expression for $\xi(t)$:

$$\dot{\xi} = -\xi + \dot{y}_2 \tag{47}$$

which can be used for analysis purposes. After differentiating the following nonnegative function:

$$V_n = V + \frac{1}{2}k_v\xi^2 \tag{48}$$

with respect to time along the new closed-loop system (i.e., use (47) and (44) instead of (24)) where $V(t)$ was defined in (35), we can use the same steps of the proof of Theorem 1 to arrive at the following expression:

$$\dot{V}_n = -\dot{y}^T F^* \dot{y} - k_v\xi^2 - \dot{y}_1 G_1^*(y_d) \tag{49}$$

The result of Theorem 1 now directly follows by applying the same steps in the proof of Theorem 1 to (49) as illustrated by the development following the expression given by (38).

4. Simulation Results

The acrobot configurations defined in (1) and (16) were simulated using the parameters given in Table 1 with the viscous friction cofficients $F_d = diag\{0.5, 0, 5\}$ to validate the performance of the proposed controller.

Table 1
Acrobot Parameters

	Link 1	Link 2	Link 3
Link length (m)	0.60	0.60	0.40
Link Mass (kg)	1.95	2.70	4.76
Center of Mass (m)	0.4909	0.4300	0.3600
Inertia Values	0.12204	0.5404	0.6788

For the directly driven acrobot, the transformation matrix S defined in (10) was selected as the identity matrix. Fig. 2 illustrates the link position trajectory for the directly driven acrobot with the control gains selected as follows:

$$k_p = 15.0 \quad k_v = 3.0$$

where the desired link position for the first link is given by $q_{d1} = 90\,\text{deg}$, (i.e., $q_{d2} = -139.46\,\text{deg}$).

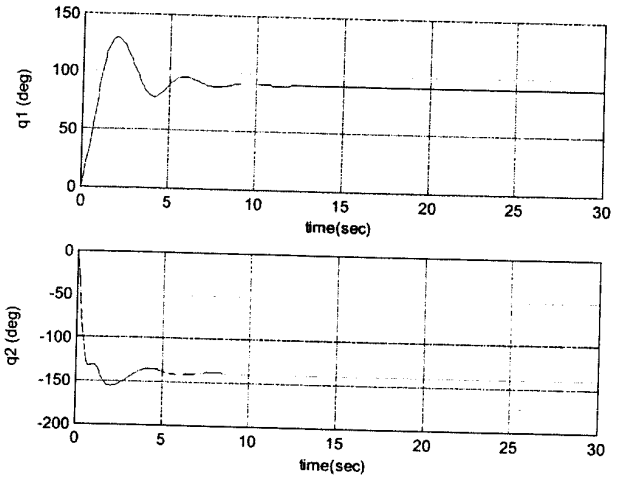

Figure 2. Simulation for directly driven acrobot with $q_{d1} = 90$ degrees, $k_p = 15.0$, and $k_v = 3.0$. After $t = 12$ sec, $q_1 = 90.0$ degrees, $q_2 = -139.46$ degrees.

For the remotely driven acrobot, the transformation matrix S defined in (10) was selected as the matrix given by (14), and the transmission vector given by (2) was selected as follows:

$$K = \begin{bmatrix} k_1 & k_2 \end{bmatrix}^T = \begin{bmatrix} -1.7308 & 2.6308 \end{bmatrix}^T \tag{50}$$

Fig. 3 illustrates the link position trajectory with the control gains selected as follows:

$$k_p = 40 \; k_v = 20$$

where the desired link position for the first link is given by $q_{d1} = 90\,\text{deg}$ (i.e., $q_{d2} = -139.46\,\text{deg}$).

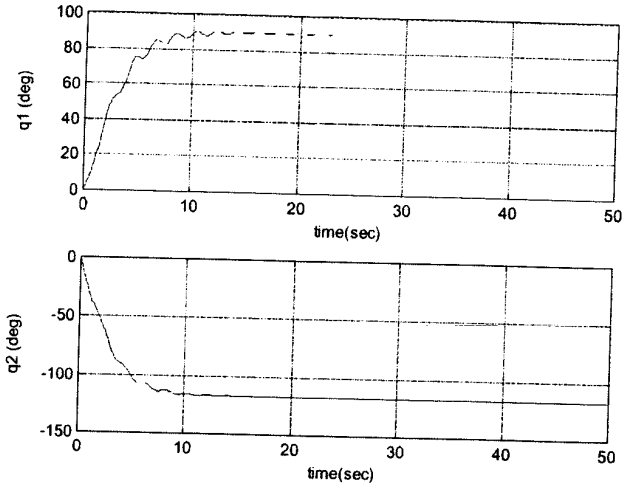

Figure 3. Simulation for remotely driven acrobot with $q_{d1} = 90$ degrees, $k_p = 40.0$, and $k_v = 20.0$. After $t = 20$ sec $q_1 = 90.0$ degrees, $q_2 = -117.88$ degrees.

5. Experimental Results

A schematic representation of the experimental set-up for the acrobot is given in Figs. 4 and 5. The links and pulleys of the acrobot were constructed from aluminium, and additional weights were placed at the end of link 2 and the counter-weight, yielding the parameter values given in Table 1. The actuator used to apply the control torque to the second link is a NSK torque controlled switch reluctance motor system, which includes a high-resolution resolver, pulse width modulated power amplifier, resolver interface, and digital control circuitry to control the motor's output torque. The motor mounted resolver is used to measure the angle between the links while a 5000 line BEI encoder is used to measure the position of the first link. Link velocities are not measured directly but are calculated via a backwards difference/filtering technique. The control software is implemented on an IBM compatible PC containing a *MultiQ* I/O board manufactured by Quanser Consulting, via the QMotor Graphical User Interface developed at Clemson University. A frequency of 1 KHz was used for data acquisition and control implementation.

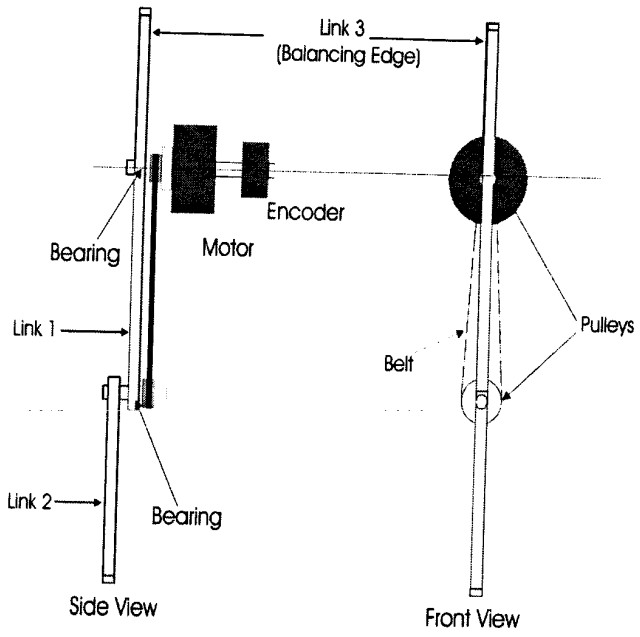

Figure 5. Acrobot set-up.

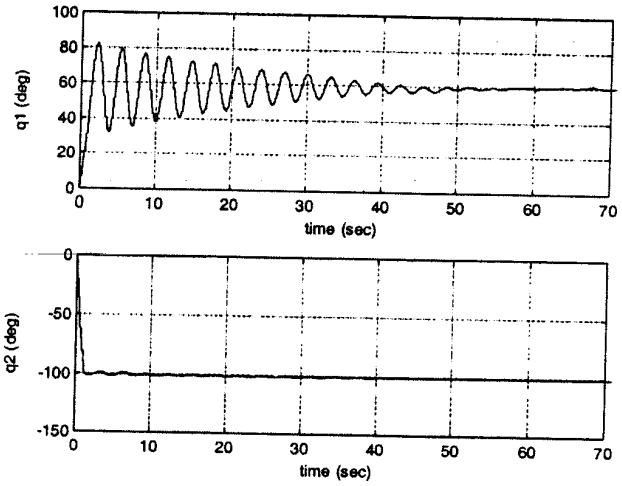

Figure 6. Experiment - $q_{d1} = 60$ degrees, $k_p = 85.75$, and $k_v = 3.65$. After $t = 55\,\text{sec}$ $q_1 = 59.92$ degrees, $q_2 = -101.22$ degrees.

Figs. 6–8 illustrate the control performance for the proposed control with desired positions of $q_{d1} = 60$ deg

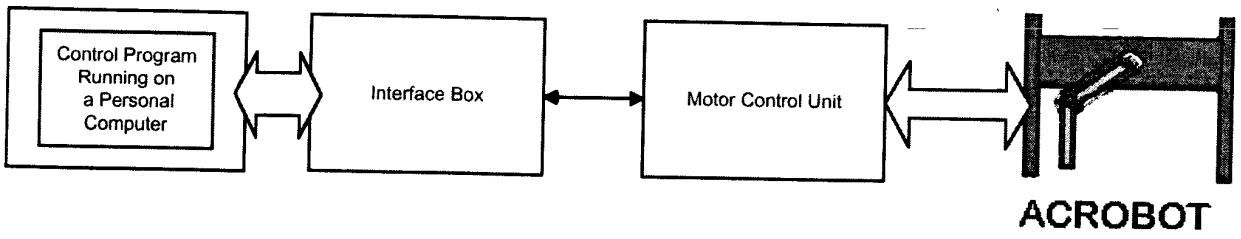

Figure 4. Experimental set-up.

(i.e., $q_{d2} = -101.16$ deg), $q_{d1} = 90$ deg (i.e., $q_{d2} = -139.46$ deg), and $q_{d1} = 180$ deg (i.e., $q_{d2} = -180$ deg). These results are as expected in that the actual position, $q_1(t)$, asymptotically goes to the desired set point q_{d1} while $q_2(t)$ asymptotically goes to the corresponding q_{d2} value.

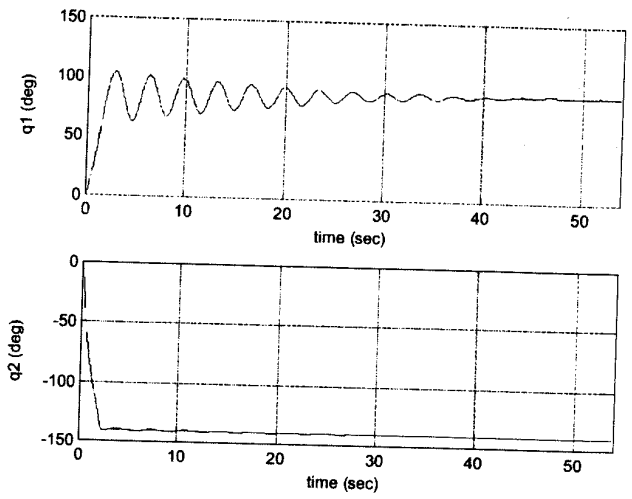

Figure 7. Experiment - $q_{d1} = 90$ degrees, $k_p = 85.75$, and $k_v = 3.65$. After $t = 45$ sec $q_1 = 89.65$ degrees, $q_2 = -140.30$ degrees.

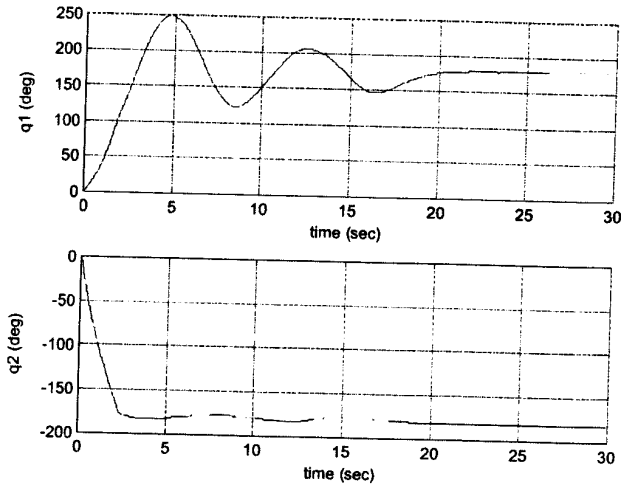

Figure 8. Experiment - $q_{d1} = 180$ degrees, $k_p = 85.75$, and $k_v = 3.65$. After $t = 20$ sec $q_1 = 180.96$ degrees, $q_2 = -181.43$ degrees.

6. Conclusion

In this paper, we present a control approach to regulate the first link of the acrobot at any desired position. Provided some sufficient conditions on the controller gains and the physical parameters are satisfied, the controller ensures that the first link is asymptotically driven to the desired set point. This control objective is achieved via the use of a desired set point position for the second link and a counter-weight attached to the first link. Both simulation and experimental results are presented to illustrate the performance of the proposed control law.

Acknowledgements

This work is supported in part by the U.S. National Science Foundation Grants DMI-9457967, DDM-931133269, CMS-9634796, ECS-9619785, DOE Grant DE-FG07-96ER14728, DOE SCUREF Fellowship, the Square D Corporation, the Union Camp Corporation, and the Gebze Institute for Advanced Technology, Gebze, Turkey.

References

[1] J. Hauser & R. Murray, Nonlinear controllers for non-integrable systems: The acrobot example, *Proc. American Control Conf.*, San Diego, CA, 1990, 669–671.

[2] M. Spong, The swing up control problem for the acrobot, *IEEE Control Systems Magazine, 15*, Feb. 1995, 49–55.

[3] S. Bortoff, Advanced nonlinear robotic control using digital signal processing, *IEEE Trans. on Industrial Electronics, 41*(1), Feb. 1994, 32–39.

[4] D. Davidson & S. Bortoff, Regulation of the acrobot, *Proc. IFAC Symp. on Nonlinear Control Systems Design*, Tahoe City, CA, June 1995, 390–395.

[5] G. Boone, Efficient reinforcement learning: Model-based acrobot control, *Proc. IEEE Int. Conf. on Robotics and Automation*, Albuquerque, NM, 1997, 229–234.

[6] G. Boone, Minimum-time control of the acrobot, *Proc. IEEE Int. Conf. on Robotics and Automation*, Albuquerque, NM, 1997, 3281–3287.

[7] M. Spong & M. Vidyasagar, *Robot dynamics and control* (New York: John Wiley & Sons Inc., 1989).

[8] J. Slotine & W.Li, Applied nonlinear control (Englewood Cliffs, NJ: Prentice Hall, 1991).

[9] T. Burg & D. Dawson, Additional notes on the TORA example: A filtering approach to eliminate velocity measurements, *IEEE Trans. on Control Systems Tech., 5*(5), September 1997, 520–523.

Appendix A

Lemma A.1: If the control gain k_p is selected according to (32) then the function $P(y)$ defined in (36) is nonnegative.

Proof: In order to show that $P(y) \geq 0$, it is sufficient to prove that $P(y)$ has a global minimum at $y(t) = y_d$ since $P(y)|_{y=y_d} = 0$. The critical points of the function $P(y)$ of (36) are obtained by setting its partial derivative equal to zero as follows:

$$\frac{\partial P(y)}{\partial y} = \begin{bmatrix} 0 \\ 0 \end{bmatrix} \tag{51}$$

After substituting (17)-(20) into (51), we obtain the following expression:

$$\begin{bmatrix} (g_1 - g_3)s_{11}\varsigma_1 + g_2(s_{11} + s_{21})\varsigma_2 \\ g_2 s_{22}\,\varsigma_2 + k_p \tanh(y_2 - y_{d2}) \end{bmatrix} = \begin{bmatrix} 0 \\ 0 \end{bmatrix} \tag{52}$$

where $\varsigma_1$and $\varsigma_2$are defined as follows:

$$\varsigma_1 = \sin(s_{11}y_1) - \sin(s_{11}y_{d1})$$

$$\varsigma_2 = \sin((s_{11} + s_{21})y_1 + s_{22}y_2) - \sin((s_{11} + s_{21})y_{d1} + s_{22}y_{d2})$$

After substituting y_{d2} defined in (25) into the top equation given in (52), we have:

$$\sin(s_{11}y_1) = \frac{1}{A}\sin\left((s_{11}+s_{21})\,y_1 + s_{22}y_2\right) \tag{53}$$

where A was defined in (27). After substituting (25) and (53) into the bottom equation given in (52), and then rewriting the resulting expression in terms of $y_1(t)$, we obtain:

$$\zeta(y_1) = \zeta_1(y_1) + \zeta_2(y_1) = 0 \tag{54}$$

where the auxiliary functions $\zeta_1(y_1)$ and $\zeta_2(y_1)$ are defined as follows:

$$\zeta_1(y_1) = s_{22}g_2A\left(\sin(s_{11}y_1) - \sin(s_{11}y_{d1})\right) \tag{55}$$

$$\zeta_2(y_1) = k_p\tanh\left(\frac{\rho}{s_{22}}\right) \tag{56}$$

and the auxiliary function $\rho(y_1)$ is defined by:

$$\rho(y_1) = \left\{\sin^{-1}\left(A\sin(s_{11}y_1)\right) - \sin^{-1}\left(A\sin(s_{11}y_{d1})\right)\right\} - (s_{11}+s_{21})\,(y_1 - y_{d1}) \tag{57}$$

Based on (55), (56), and (57), it is obvious that $y_1(t) = y_{d1}$ is a critical point of $P(y)$.

We now show that if: 1) the control gain k_p is selected according to (32), 2) the value for the counter-weight g_3 is designed to satisfy (26), and 3) the S matrix defined in (11) satisfies the condition given by (13), then $y_1(t) = y_{d1}$ is the only critical point. To this end, we first lower bound $\zeta_2(y_1)$ of (56) with the following piece-wise, continuous function denoted by $f_{pc}(y_1)$:

$$f_{pc}(y_1) = \begin{cases} \xi & y_1 \le \left(y_{d1} - \frac{\pi}{s_{11}}\right) \\ -\frac{\xi}{\frac{\pi}{s_{11}}}y_1 & \left(y_{d1} - \frac{\pi}{s_{11}}\right) < y_1 \le y_{d1} \\ \frac{\xi}{\frac{\pi}{s_{11}}}y_1 & y_{d1} < y_1 < \left(y_{d1} + \frac{\pi}{s_{11}}\right) \\ \xi & y_1 \ge \left(y_{d1} + \frac{\pi}{s_{11}}\right) \end{cases} \tag{58}$$

with:

$$\xi = k_p\tanh\left\{\frac{-1}{s_{22}}\left[2\sin^{-1}\left(A\sin(s_{11}y_{d1})\right) + (s_{11}+s_{21})\frac{\pi}{s_{11}}\right]\right\}$$

From the structure of (58), it is straightforward to see that:

$$|f_{pc}(y_1)| \le |\zeta_2(y_1)| \tag{59}$$

Based on the form of (58), we now show that $P(y_1)$ has only one critical point. First, we prove that the slope of $f_{pc}(y_1)$ is greater than the slope of $\zeta_1(y_1)$ for the "unsaturated" region given by $\left(y_{d1} - \frac{\pi}{s_{11}}\right) < y_1 < \left(y_{d1} + \frac{\pi}{s_{11}}\right)$. The slope of the "unsaturated" region of $f_{pc}(y_1)$, and the slope of $\zeta_1(y_1)$ are found by taking the partial derivative with respect to $y_1(t)$ as follows:

$$\frac{\partial}{\partial y_1}f_{pc}(y_1) = \begin{cases} -\frac{\xi}{\frac{\pi}{s_{11}}} & \left(y_{d1} - \frac{\pi}{s_{11}}\right) < y_1 \le y_{d1} \\ \frac{\xi}{\frac{\pi}{s_{11}}} & y_{d1} < y_1 < \left(y_{d1} + \frac{\pi}{s_{11}}\right) \end{cases} \tag{60}$$

where the auxiliary variable ξ was previously defined in (58).
And:

$$\frac{\partial}{\partial y_1}\zeta_1(y_1) = s_{11}s_{22}g_2A\cos(s_{11}y_1) \tag{61}$$

To show that the slope of $f_{pc}(y_1)$ is greater than the slope of $\zeta_1(y_1)$, we can now use (60) and (61) to formulate the following two inequalities:

$$-k_p\tanh\left\{\frac{-1}{s_{22}}\left[2\sin^{-1}\left(A\sin(s_{11}y_{d1})\right) + (s_{11}+s_{21})\frac{\pi}{s_{11}}\right]\right\} > \pi s_{22}g_2A\cos(s_{11}y_1) \tag{62}$$

for the region given by $\left(y_{d1} - \frac{\pi}{s_{11}}\right) < y_1 \le y_{d1}$ and:

$$k_p\tanh\left\{\frac{-1}{s_{22}}\left[2\sin^{-1}\left(A\sin(s_{11}y_{d1})\right) - (s_{11}+s_{21})\frac{\pi}{s_{11}}\right]\right\} > \pi s_{22}g_2A\cos(s_{11}y_1) \tag{63}$$

for the region given by $y_{d1} < y_1 < \left(y_{d1} + \frac{\pi}{s_{11}}\right)$. Based on the expressions given by (62) and (63), we can utilize the fact that:

$$\left|\sin^{-1}(\cdot)\right| \le \frac{\pi}{2} \tag{64}$$

in conjunction with the conditions given in (26) and (13) to determine the following sufficient condition on k_p:

$$k_p > \gamma_1 = \left|\pi\,(g_3 - g_1)\left(\frac{s_{11}s_{22}}{s_{11}+s_{21}}\right)\right| \tag{65}$$

to ensure that the slope of $f_{pc}(y_1)$ is greater than the slope of $\zeta_1(y_1)$. From a graph of $f_{pc}(y_1)$ and $\zeta_1(y_1)$, it is easy to see that if k_p is selected according to (65) then $f_{pc}(y_1)$ and $\zeta_1(y_1)$ will intersect only at one point in the region given by $\left(y_{d1} - \frac{\pi}{s_{11}}\right) < y_1 \le \left(y_{d1} + \frac{\pi}{s_{11}}\right)$; hence, we can now use (54) and (59) to show that $P(y_1)$ has only one critical point for the region given by $\left(y_{d1} - \frac{\pi}{s_{11}}\right) < y_1 \le \left(y_{d1} + \frac{\pi}{s_{11}}\right)$.

We now illustrate how k_p can be selected to eliminate the possibility of critical points from the regions given by $y_1 \le \left(y_{d1} - \frac{\pi}{s_{11}}\right)$ and $y_1 \ge \left(y_{d1} + \frac{\pi}{s_{11}}\right)$. That is, since the $f_{pc}(y_1)$ function saturates in this region, we can select k_p greater than the maximum value of $\zeta_1(y_1)$ as follows:

$$k_p > \gamma_2 = \left|2\,(g_3 - g_1)\left(\frac{s_{11}s_{22}}{s_{11}+s_{21}}\right)\right| \tag{66}$$

to ensure that $f_{pc}(y_1)+\zeta_1(y_1) \neq 0$ for the regions given by $y_1 \leq \left(y_{d1}-\frac{\pi}{s_{11}}\right)$ and $y_1 \geq \left(y_{d1}+\frac{\pi}{s_{11}}\right)$. Hence, we can use (54) and (59) to show that $\zeta(y_1)$ does not have any critical points in the regions given by $y_1 \leq \left(y_{d1}-\frac{\pi}{s_{11}}\right)$ and $y_1 \geq \left(y_{d1}+\frac{\pi}{s_{11}}\right)$. It is obvious from (65) and (66) that $\gamma_1 > \gamma_2$ and if k_p is chosen as:

$$k_p > \gamma_1 \tag{67}$$

then the only critical point for $\zeta(y_1)$ is at $y_1(t) = y_{d1}$. Note that (32) is a sufficient condition for (67).

We now show that if: 1) the control gain k_p is selected according to (32), and 2) the value for the counter-weight g_3 is designed to satisfy (26), then the critical point $y_1(t) = y_{d1}$ is a global minimum. In order to prove that the critical point $y_1(t) = y_{d1}$ is a global minimum, it is necessary to show that the matrix $\frac{\partial^2 P(y)}{\partial y^2}\Big|_{y=y_d}$ is positive definite. The ij-th elements of the matrix $\frac{\partial^2 P(y)}{\partial y^2} \in \Re^{2\times 2}$ are calculated by taking the partial derivative of (52) as shown below:

$$\left(\frac{\partial^2 P(y)}{\partial y^2}\right)_{11} = (g_1-g_3)\, s_{11}^2 \cos(s_{11}y_1)$$
$$+g_2\,(s_{11}+s_{21})^2 \cos((s_{11}+s_{21})\,y_1 + s_{22}y_2) \tag{68}$$

$$\left(\frac{\partial^2 P(y)}{\partial y^2}\right)_{12} = \left(\frac{\partial^2 P(y)}{\partial y^2}\right)_{21}$$
$$= g_2 s_{22}\,(s_{11}+s_{21}) \cos((s_{11}+s_{21})\,y_1 + s_{22}y_2) \tag{69}$$

$$\left(\frac{\partial^2 P(y)}{\partial y^2}\right)_{22} = g_2 s_{22}^2 \cos((s_{11}+s_{21})\,y_1 + s_{22}y_2)$$
$$+k_p\left(1-\tanh^2(y_2-y_{d2})\right) \tag{70}$$

To show that the matrix $\frac{\partial^2 P(y)}{\partial y^2}\Big|_{y=y_d}$ is positive definite, we must show that:

$$\left(\frac{\partial^2 P(y)}{\partial y^2}\right)_{11}\Big|_{y=y_d} > 0$$
$$\Delta \triangleq \left[\left(\frac{\partial^2 P(y)}{\partial y^2}\right)_{11}\left(\frac{\partial^2 P(y)}{\partial y^2}\right)_{22}\right.$$
$$\left.-\left(\frac{\partial^2 P(y)}{\partial y^2}\right)_{12}\left(\frac{\partial^2 P(y)}{\partial y^2}\right)_{12}\right]\Big|_{y=y_d} > 0 \tag{71}$$

To validate the top inequality in (71), we set y_1 equal to y_{d1} and substitute y_{d2} from (25) for y_2 into (68) to yield:

$$\left(\frac{\partial^2 P(y)}{\partial y^2}\right)_{11}\Big|_{y=y_d} = (g_1-g_3)\, s_{11}^2 \cos(s_{11}y_{d1})$$
$$+g_2\,(s_{11}+s_{21})^2 \cos(\sin^{-1}\{A\sin(s_{11}y_{d1})\}) > 0 \tag{72}$$

where A was defined in (27). After some algebraic manipulations, we can rewrite (72) in the following manner:

$$\left(\frac{\partial^2 P(y)}{\partial y^2}\right)_{11}\Big|_{y=y_d} = \sqrt{1-[A\sin(s_{11}y_{d1})]^2}$$
$$-A\left(\frac{s_{11}}{s_{11}+s_{21}}\right)\cos(s_{11}y_{d1}) > 0 \tag{73}$$

After squaring both sides of the inequality given by (73), we can use (26) and (13) to show that $\left(\frac{\partial^2 P(y)}{\partial y^2}\right)_{11}\Big|_{y=y_d} > 0$. To validate the bottom inequality in (71), we substitute (68), (69), and (70) into (71), set y_1 equal to y_{d1}, and substitute y_{d2} from (25) for y_2, and simplify the resulting expression to obtain the following inequality:

$$\Delta = k_p\left[\left(\frac{\partial^2 P(y)}{\partial y^2}\right)_{11}\Big|_{y=y_d}\right]$$
$$-s_{11}^2 s_{22}^2\,(g_3-g_1)\,g_2\cos(s_{11}y_{d1})$$
$$\cos((s_{11}+s_{21})\,y_1 + s_{22}y_2) > 0 \tag{74}$$

where (72) has been utilized to substitute for $\left(\frac{\partial^2 P(y)}{\partial y^2}\right)_{11}$. From (74) and (72), we can select k_p as follows:

$$k_p > \gamma_3 = \left|\frac{s_{11}^2 s_{22}^2\,(g_3-g_1)\,g_2}{\varrho}\right| \tag{75}$$

to validate the bottom inequality given in (75). Note that (32) is a sufficient condition for (75). QED

Biographies

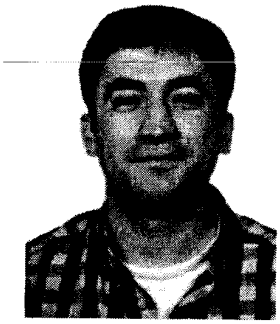

Erkan Zergeroglu graduated from Ataturk Anatolian High School of Ankara in 1988, received his B.Sc.degree in electrical engineering in 1992 from Hacettepe University, and his M.Sc. degree from the Middle East Technical University in 1996. Currently he is a Ph.D. student in the Clemson University Robotics and Mechatronics Laboratory. His research interests are nonlinear control of electromechanical systems with parametric uncertainty, control of underactuated systems, and applied robotics.

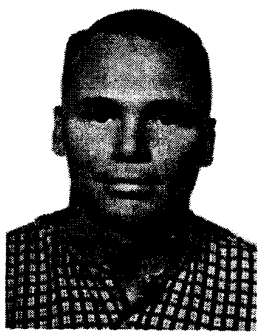

Warren Dixon received his B.Sc. degree in 1994 from the Department of Electrical and Computer Engineering, Clemson University, Clemson, South Carolina and his M.Sc. of Engineering degree in 1997 from the Department of Electrical and Computer Engineering, University of South Carolina, Columbia, South Carolina. He returned to Clemson University where he is currently pursuing a Ph.D. degree. As a student in the Robotics and Mechatronics Group at Clemson University, his research is focused on nonlinear based robust and adaptive control techniques with application to electromechanical systems, including wheeled mobile robots and robot manipulators.

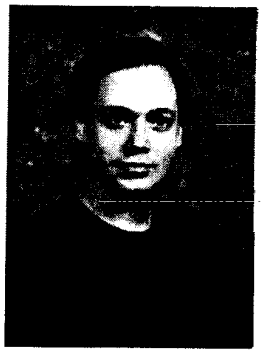

Darren M. Dawson received his Associate Degree in Mathematics from Macon Junior College in 1982 and his B.S. Degree in electrical engineering from the Georgia Institute of Technology in 1984. He then worked for Westinghouse as a Control Engineer from 1985 to 1987. In 1987, he returned to the Georgia Institute of Technology where he received his Ph.D. degree in electrical engineering in March, 1990. In July 1990, he joined the Electrical and Computer Engineering Department and the Center for Advanced Manufacturing (CAM) at Clemson University, where he currently holds the position of Professor. Under the CAM director's supervision, he currently leads the Robotics and Manufacturing Automation Laboratory, which is jointly operated by the Electrical and Mechanical Engineering departments. His main research interests are in the fields of nonlinear-based robust, adaptive, and learning control with application to electromechanical systems including robot manipulators, motor drives, magnetic bearings, flexible cables, flexible beams, and high-speed transport systems.

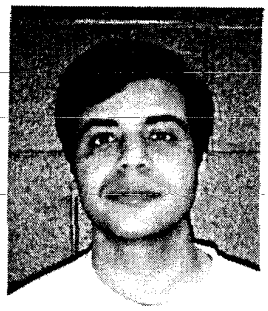

Aman Behal received his M.Sc. degree in electrical engineering from Indian Institute of Technology, Bombay in 1996. He is currently working towards a Ph.D in Controls and Robotics at Clemson University. His research focuses on the control of nonlinear systems with special interest in motor control and underactuated systems.